

A review and comparison of different methods to determine the series resistance of solar cells

D. Pysch^{a,*}, A. Mette^a, S.W. Glunz^a

^a*Fraunhofer Institute for Solar Energy Systems, Heidenhofstr. 2, D-79110 Freiburg, Germany*

Received 26 January 2007; accepted 16 May 2007

Available online 20 July 2007

Abstract

This work presents a review of five different methods to determine the lumped series resistance R_s of solar cells and an experimental investigation of these to find the most reliable and robust method(s) for cell characterization under operating conditions. The methods under consideration are: fitting of the two-diode equation function to a dark IV -curve, comparison of a one-sun with a dark IV -curve, comparison of a Suns- V_{OC} with a one-sun IV -curve, comparison of two or more IV -curves measured at different illumination intensities, and computation of the area under a one-sun IV -curve. Firstly, for a quantitative evaluation, all series resistance values were plotted against the fill factor FF of the corresponding cell. The accuracy of the methods is quantified using a wide range of solar cells. Secondly, the robustness of the methods in the presence of other FF-limitations such as shunts is also explored. The results and the interpretation of a first analysis of small $2 \times 2 \text{ cm}^2$ solar cells of the integration method led to a successful improvement of this method, which was proven by a second measurement. All the conducted investigations led us to the conclusion that of these five methods under consideration, the illumination intensity variation, the comparison of a Suns- V_{OC} with a one-sun IV -curve, and the modified comparison of a one-sun IV -curve with a dark IV -curve method are the most reliable and robust ways to determine the series resistance under operating conditions.

© 2007 Elsevier B.V. All rights reserved.

Keywords: Solar cell; Characterization; Series resistance

1. Introduction

Solar cells are known to be high current and low voltage power generators. Today $15.6 \times 15.6 \text{ cm}^2$ solar cells are able to produce currents up to 8.2 A. Since the area and consequently the finger length of industrial solar cells has increased steadily during the past years, the power loss due to the series resistance has risen because of the increase in finger length and current. Therefore, it becomes more and more important to determine the series resistance as accurately as possible, to get a reliable characterization in both, industrial production for quality control and also in solar cell development labs to determine the amount of this loss mechanism as accurately as possible. Thus, keeping the

series resistance as low as possible is certainly of major importance.

It is necessary to distinguish two types of series resistance effects: firstly, series resistance under illuminated conditions, $R_{S,\text{light}}$; and secondly, without illumination, $R_{S,\text{dark}}$ [1]. This distinction is essential due to the different current flow pattern in each state [2]. In the illuminated state, electrons are generated homogeneously over the whole cell area and also diffuse almost homogeneously to the emitter. Due to this fact a larger lateral electron flow in the emitter can be observed for the illuminated state, and this is one of the main reasons for higher $R_{S,\text{light}}$ value compared with $R_{S,\text{dark}}$. The series resistance under illuminated conditions $R_{S,\text{light}}$ is the more interesting value for solar cell characterization, due to measuring under real operating conditions. Here, we review four different experimental methods to determine the illuminated series resistance $R_{S,\text{light}}$, and one for $R_{S,\text{dark}}$ measurements, and compare them to find the most reliable and accurate measurement.

*Corresponding author. Tel.: +49 76145885366; fax: +49 7614588250.
E-mail address: damian.pysch@ise.fraunhofer.de (D. Pysch).

2. Review of R_S determination methods

In the following, five R_S -determination methods are presented in detail [2–11].

2.1. Fitting of the two-diode equation function to the dark IV -curve

This method is based on an analytical description of a solar cell by the two-diode model (see Eq. (1)):

$$J = J_{01} \left(\exp \left(\frac{q(V - JR_{S,\text{dark}})}{n_1 k_B T} \right) - 1 \right) + J_{02} \left(\exp \left(\frac{q(V - JR_{S,\text{dark}})}{n_2 k_B T} \right) - 1 \right) + \frac{V - JR_{S,\text{dark}}}{R_P} - J_{\text{Ph}}, \quad (1)$$

where J_{01} and J_{02} are recombination current densities of the emitter/base and the space-charge region, respectively, J_{Ph} is the photo-generated current density, R_P is the parallel resistance and $n_1 = 1$ and $n_2 = 2$ are ideality factors. The procedure to determine the series resistance is as follows: after measuring the dark IV -curve, the two-diode equation is fitted to the measured IV -points (see Fig. 1). The series resistance $R_{S,\text{dark}}$ is extracted from the upper voltage part (0.6–0.8 V), where the power loss due to the series resistance is most significant.

2.2. Comparison of the one-sun with the dark IV -curve

The measurement principle of this method for $R_{S,\text{light}}$ determination is based on a voltage difference at the maximum power point (index: mpp) of the one-sun IV - and the dark IV -curve, which is shifted by the short circuit current density J_{SC} (see Fig. 2), as proposed by A. Aberle

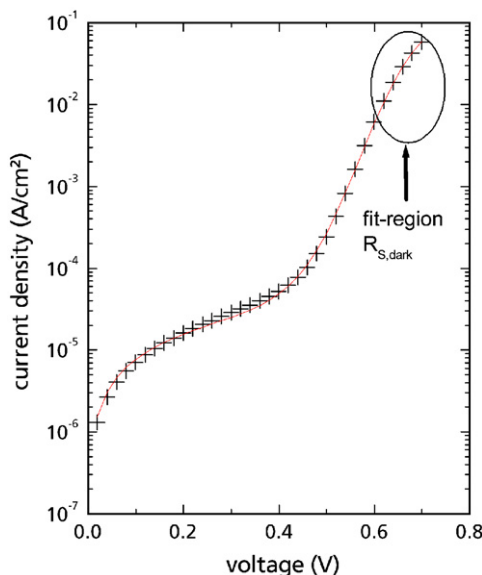


Fig. 1. Dark IV -curve and the fit function of the two-diode model.

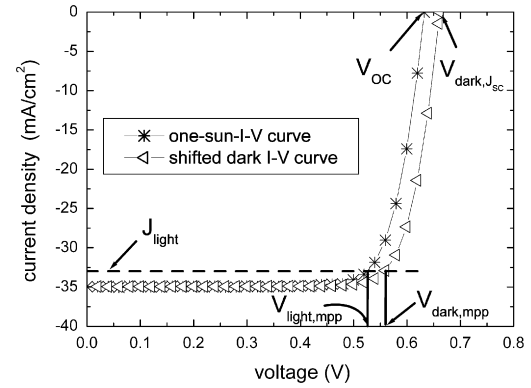


Fig. 2. One-sun and J_{SC} shifted dark IV measurements.

(see Refs. [2,3]):

$$R_{S,\text{light_dark}} = \frac{V_{\text{dark,mpp}} - V_{\text{light,mpp}}}{|J_{\text{mpp}}|}. \quad (2)$$

Eq. (2) assumes that the active dark series resistance at $V_{\text{dark,mpp}}$ can be neglected for the shifted dark IV -curve, since the current density at this point ($J_{\text{SC}} - J_{\text{mpp}}$) is low. As shown by Dicker the error due to this assumption can, however, be larger than 5% relative for typical solar cells [4]. He suggested a way to take the dark series resistance losses into account:

$$R_{S,\text{light_dark,corr}} = \frac{V_{\text{dark,mpp}} - V_{\text{light,mpp}} - (|J_{\text{SC}}| - |J_{\text{mpp}}|)R_{S,\text{dark}}}{|J_{\text{mpp}}|}, \quad (3)$$

where $R_{S,\text{dark}}$ represents the dark series resistance which is calculated by

$$R_{S,\text{dark}} = \frac{V_{\text{dark},J_{\text{SC}}} - V_{\text{OC}}}{|J_{\text{SC}}|}. \quad (4)$$

Since the open-circuit voltage under illuminated conditions V_{OC} is series resistance-free, the voltage difference between $V_{\text{dark},J_{\text{SC}}}$ and V_{OC} is caused by the dark series resistance (see Fig. 2), with $V_{\text{dark},J_{\text{SC}}}$ representing the voltage on the dark IV -curve at the current density of J_{SC} .

2.3. Comparison of the Suns- V_{oc} or the $J_{\text{SC}}-V_{\text{OC}}$ curve with the one-sun IV -curve

This method is based on the fact that the $J_{\text{SC}}-V_{\text{OC}}$ (equivalently the Suns- V_{OC})-curve is free from series resistance effects. Thus, it is possible to calculate the series resistance using the following equation suggested by Wolf in 1963 [5]:

$$R_{S,\text{Suns}V_{\text{OC}}} = \frac{\Delta V}{J_{\text{mpp}}}, \quad (5)$$

where ΔV is the voltage difference between the series-resistance-free $J_{\text{SC}}-V_{\text{OC}}$ curve and the series-resistance-affected one-sun IV -curve determined at the mpp of the one-sun IV -curve. This ΔV is divided by the current density

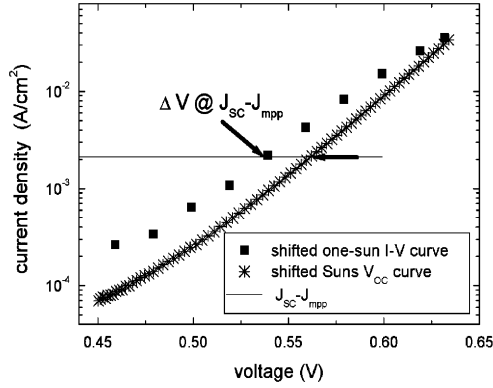


Fig. 3. This figure shows a by J_{SC} -shifted Suns- V_{OC} and one-sun IV measurement.

at that point (mpp). Fig. 3 shows a one-sun and a Suns- V_{OC} curve, which yields the same information as the J_{SC} - V_{OC} curve, measured for the same solar cell. The Suns- V_{OC} measurement was performed by taking the open-circuit voltage values V_{OC} of a solar cell under variation of the light intensity by a flash and calculating the corresponding values of the current density over a calibrated reference cell with the known short circuit current density J_{SC} at one-sun illumination [6]. This is a quick method to determine the J_{SC} - V_{OC} curve of a solar cell.

2.4. Comparison of two or more IV -curves measured at different illumination intensities

Measuring the IV -curves at two different illumination levels results in two shifts between them. The first shift is in voltage which is caused by the smaller series resistance loss, at a lower light intensity $\Delta V = R_{S,light} \Delta J_{SC}$, with ΔJ_{SC} the difference in the two short-circuit current densities. The second shift is in current density, because the incident illumination power is proportional to the photo generated current (see Fig. 4) [5,7]. The method to determine $R_{S,light}$ from these curves was first suggested by Swanson in 1960 [10]. The IV point [J_i, V_i] that lies at a fixed distance ΔJ from the short-circuit current (e.g. $J_i = J_{SC} - \Delta J$) is marked on each curve. The European standard suggests choosing the parameter ΔJ in a way that the corresponding voltage value V_i from the one-sun IV -curve should be slightly above the voltage at the maximum power point V_{mpp} [8]. It is more accurate to compare three (or more) IV -curves at different illumination levels and connect the resulting IV -points by a linear fit function. The magnitude of the inverted value of the corresponding slope leads to the series resistance:

$$R_{S,int,var.} = \left| \frac{\Delta V}{\Delta J_{SC}} \right|. \quad (6)$$

We suggest choosing three illumination intensities: (1) slightly above, (2) directly at and (3) slightly below one-sun intensity. This is important to guarantee measurement

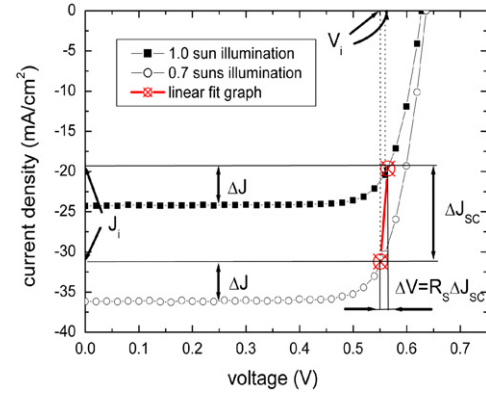


Fig. 4. Two IV -curves of the same solar cell under different illumination intensities.

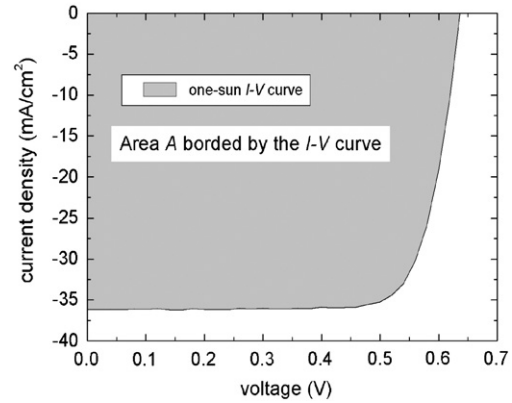


Fig. 5. A one-sun IV -curve is presented of which the voltage integral from zero to short-circuit current density is calculated to determine the series resistance.

conditions as close as possible to the actual working state of the solar cell, and thus to minimize the influence of the dependence of the series resistance on the illumination intensity [14].

2.5. Computation of the area A under an IV -curve

In 1982, Araujo suggested a very elegant way to determine the series resistance, in which only one IV -curve is needed to determine $R_{S,light}$ [11]. This method is based on the R_S -modified one-diode model equation:

$$J(V) = J_0 \left(\exp \left(\frac{V + JR_S}{k_B T} \right) - 1 \right) - J_{Ph}. \quad (7)$$

This implicit equation in current density is solved for the voltage V and then integrated from zero to short-circuit current density to obtain the area A bordered by the one-sun IV -curve (Fig. 5),

$$A = \int_{J_2=0}^{J_1=J_{SC}} V(J) dJ. \quad (8)$$

Eq. (8) can now be solved for the series resistance and simplified to

$$R_{S,\text{integral}} = 2 \cdot \left(\frac{V_{oc}}{J_{sc}} - \frac{A}{J_{sc}^2} - \frac{k_B T}{q} \cdot \frac{1}{J_{sc}} \right). \quad (9)$$

3. Experimental details

For an evaluation of the different R_S determination methods two different solar cell sizes were fabricated and characterized. In the first batch $2 \times 2 \text{ cm}^2$ silicon solar cells were processed on 4" FZ p-type wafers, with a base resistivity of $0.5 \Omega \text{ cm}$. The process sequence was similar to that of standard industrial solar cells: The wafers were wet-chemical textured, had a POCl_3 -diffused emitter of $50 \Omega/\text{sq.}$, a SiN_x antireflection coating and a screen-printed aluminum rear side. Fine metal lines (finger separation distance 1.9 mm and width $90 \mu\text{m}$) were screen printed on the front side using conventional silver screen-printing paste. Finally, the wafers were fired in a fast firing belt furnace, edge isolated and the contact fingers were thickened by light-induced silver plating [12]. The second batch of $12.5 \times 12.5 \text{ cm}^2$ Cz-silicon solar cells with a $1\text{--}3 \Omega \text{ cm}$ p-type base resistivity was processed similar to the first batch, except from the front side contact, for which a hotmelt screen-printing paste was used (finger distance 2.2 mm and width $100 \mu\text{m}$). With the just mentioned parameters we calculated an estimated value for the components of the series resistance: $R_{S,\text{base}} = 0.01 \Omega \text{ cm}^2$, $R_{S,\text{emitter}} = 0.14 \Omega \text{ cm}^2$, $R_{S,\text{contact}} = 0.1 \Omega \text{ cm}^2$, $R_{S,\text{finger}} = 0.14 \Omega \text{ cm}^2$, $R_{S,\text{bus}} = 0.02 \Omega \text{ cm}^2$ (for the 4 cm^2 cells), and for the 150 cm^2 cells $R_{S,\text{base}} = 0.04 \Omega \text{ cm}^2$, $R_{S,\text{emitter}} = 0.2 \Omega \text{ cm}^2$, $R_{S,\text{contact}} = 0.1 \Omega \text{ cm}^2$, $R_{S,\text{finger}} = 0.23 \Omega \text{ cm}^2$, $R_{S,\text{bus}} = 0.03 \Omega \text{ cm}^2$ (for the 4 cm^2 cells). Thus, the measured series resistance values should be in the range of $R_S = 0.41 \Omega \text{ cm}^2$ for the 4 cm^2 cells (in very good agreement with the experiment, see Fig. 7) and $R_S = 0.6 \Omega \text{ cm}^2$ for the 150 cm^2 cells (also in good agreement with the experiment; the R_S values are slightly underestimated by the calculation; this can possibly be justified by neglecting possible interruption of the contact fingers in the calculation).

The IV -curves of 49 (4 cm^2) and 30 (150 cm^2) solar cells were measured at three different illumination levels (using a steady-state sun simulator): 1.0 , 0.8 , 0.7 suns, in addition to the dark IV and the Suns- V_{oc} curve. The reduction of the illumination intensity was realized by using appropriate shading filters; therefore, the light spectrum stays approximately unchanged for all considered intensities. The Suns- V_{oc} measurements were taken as proposed by Sinton [6], using the generalized analysis type, and the temperature correction was to 25°C . Based on these data the solar cell parameters, FF, η (efficiency), R_p , J_{01} , J_{02} , the four different $R_{S,\text{light}}$, and the $R_{S,\text{dark}}$ values were determined. The measurement uncertainties of the used sun simulator in voltage (2 mV) and current density (0.6 mA/cm^2) result in an uncertainty in the series resistance of $0.11 \Omega \text{ cm}^2$

which is significant lower than the uncertainty of the linear fit procedure of Section 4.2.

4. Results

In this section the five different methods are compared experimentally in order to find the most accurate (Sections 4.1 and 4.2) and robust (Section 4.3) method for solar cell characterization.

4.1. Simulation of a FF vs. R_S graph

In this paragraph the simulation of a FF vs. R_S graph is shown and discussed to motivate the procedure of Section 4.2 in which the accuracy of the five R_S -methods will be checked by comparing the linear fit parameter with calculated mean values.

Based on Eq. (1) an FF vs. R_S plot was generated under variation of the series resistance and for three different photo generation current densities J_{Ph} (representing a multi-, mono-crystalline and a high-efficiency silicon solar cell, see Fig. 6). All remaining parameters of Eq. (1) were kept constant. In the relevant FF-range for industrial solar cells ($\text{FF} > 70\%$) Fig. 6 shows a perfect linear dependency between the fill factor and the series resistance. The linear-fit parameters for the slopes of each J_{Ph} are very similar, so we can deduce a rule of thumb for silicon solar cells: The fill factor changes by 5% absolute per change of the series resistance by $1 \Omega \text{ cm}^2$.

Since this simulation shows that it is possible to linear fit the FF vs. R_S graph it should be also justified applying a linear fit to a measured FF vs. R_S graph.

4.2. Fill factor dependence on R_S

By taking a closer look at the measured cell parameters of the solar cells of both batches, it becomes evident that V_{oc} , J_{sc} and J_{mpp} (the current density at the maximum power point) are very similar for each batch, and can be

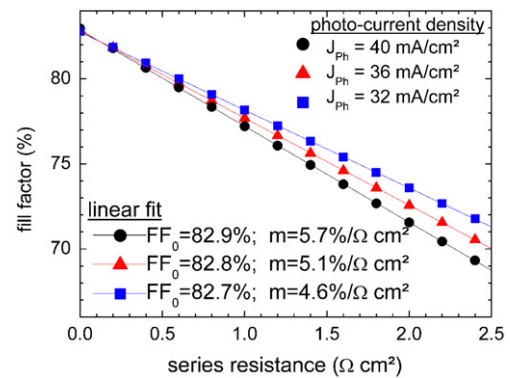


Fig. 6. FF vs. R_S -simulation based on the two-diode Equation (1) for three different photo-generated current densities fitted by a linear function. The parameters $n_1 = 1$, $n_2 = 2$, $J_{01} = 1.2 \times 10^{-12} \text{ mA cm}^{-2}$, $J_{02} = 1.2 \times 10^{-9} \text{ mA cm}^{-2}$ and $R_p = 10 \text{ k}\Omega \text{ cm}^2$ were kept constant.

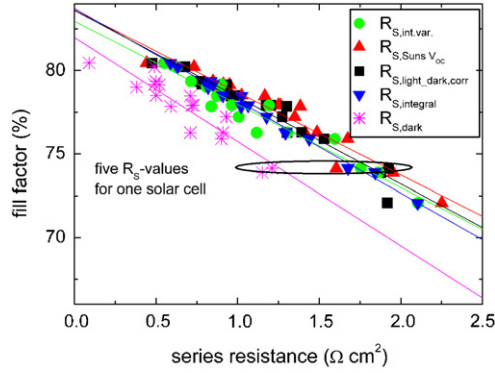


Fig. 7. Plotted are FFs values of 17 of the 49 measured solar cells (4 cm^2) which satisfy the prerequisite that their J_{mpp} can be approximated as constant over the four different $R_{\text{S,light}}$ and a $R_{\text{S,dark}}$ value. Hence, it is possible to approach the measured points by a linear fit for this FF range.

assumed as approximately constant for cells with FF's higher than 72% and $R_{\text{P}} > 2\text{ k}\Omega$ (e.g. for the 4 cm^2 batch, we obtained the following mean values: $J_{\text{mpp}} = 32.6 \pm 1.3\text{ mA/cm}^2$, $V_{\text{OC}} = 633.6 \pm 2.0\text{ mV}$ and $J_{\text{SC}} = 35.6 \pm 0.5\text{ mA/cm}^2$). We plotted 17 of the 49 measured cells (the 17 cells fulfill the above-mentioned prerequisites) resulting in one fill factor, plotted against five values of R_{S} ; this forms a horizontal line of five R_{S} points for each FF value for each solar cell (see Fig. 7). For these selected cells it is possible to approximate a plot of FF vs. $R_{\text{S,light}}$ by a linear fit (see Fig. 7).

Since a change of R_{S} mainly creates a voltage drop and not a change in current [13] and J_{mpp} is approximately constant for all cells in this experiment, an additional series resistance ΔR_{S} will cause an additional voltage drop ΔV at J_{mpp} :

$$\Delta V_{\text{at } J_{\text{mpp}}} = J_{\text{mpp}} \Delta R_{\text{S}}. \quad (10)$$

Using the definition of FF we can calculate the FF-difference for solar cells with different series resistance values (at mpp):

$$\begin{aligned} \Delta \text{FF} = \text{FF}_2 - \text{FF}_1 &= \frac{J_{\text{mpp}}(V_1 + \Delta V_{\text{at } J_{\text{mpp}}}) - J_{\text{mpp}} V_1}{V_{\text{OC}} J_{\text{SC}}} \\ &= \frac{J_{\text{mpp}}^2 \Delta R_{\text{S}}}{V_{\text{OC}} J_{\text{SC}}}. \end{aligned} \quad (11)$$

Therefore it is possible to predict the slope m of the linear fit, by applying Eqs. (10) and (11) and dividing the whole term by ΔR_{S} :

$$m = \frac{\Delta \text{FF}}{\Delta R_{\text{S}}} = \frac{J_{\text{mpp}}^2}{V_{\text{OC}} J_{\text{SC}}}. \quad (12)$$

The equation for the fit is $\text{FF}(R_{\text{S}}) = \text{FF}_0 - m_{\text{fit}} R_{\text{S}}$, where FF_0 is the ideal FF when $R_{\text{S}} = 0\text{ }\Omega\text{ cm}^2$, of course under the assumption of constant J_{mpp} , J_{SC} and V_{OC} , whereas FF_0 and m_{fit} should be unique. Nevertheless, we can apply the

definition in Eq. (12) to each solar cell to determine an average value and standard deviation for both batches:

$$\bar{m}_{4.0\text{ cm}^2} \cong 4.9 \pm 0.6 \frac{\%}{\Omega\text{ cm}^2} \quad \text{and} \quad \bar{m}_{150\text{ cm}^2} \cong 4.9 \pm 0.1 \frac{\%}{\Omega\text{ cm}^2}. \quad (13)$$

The standard deviation for the 150 cm^2 solar cells is much lower than the one for the 4 cm^2 cells. A possible reason for this distinction could be, that the large-area cells have a much higher current flow, and are therefore not as sensitive to possible measurement uncertainties of all determined values. The FF-axis intersection point $\text{FF}_{0,\text{fit}}$ can be determined experimentally by measuring the pseudo fill factor PFF of the $R_{\text{S,light}}$ -free Suns- V_{OC} IV-curve. The following values have been determined:

$$\overline{\text{PFF}}_{4.0\text{ cm}^2} = 83.4 \pm 0.6\% \quad \text{and} \quad \overline{\text{PFF}}_{150\text{ cm}^2} = 82.8 \pm 0.2\%. \quad (14)$$

Again, the standard deviation for the large-area cells is much lower.

The next step is to fit separately the different sets of FF vs. R_{S} points obtained with the different methods. By a comparison between the respective m_{fit} and $\text{FF}_{0,\text{fit}}$ to the expected mean values given by Eqs. (13) and (14), we can establish the accuracy of each method (see Fig. 7 and Table 1).

One can draw the following three conclusions for the 4 cm^2 batch.

- There is a huge difference between the dark and the illuminated series resistance. The dark series resistance amounts in most cases only to half of the light series resistance and is, therefore, not useful for solar cell characterization.
- All four $R_{\text{S,light}}$ determination methods result in very similar values (within the statistical uncertainty range, Table 1), and are, therefore, equally good for small size solar cell investigations. Nevertheless, the integration method shows the biggest difference between the

Table 1

Slopes and FF-axis intersection points determined by a linear fit to the FF vs. R_{S} plot, in comparison with calculated mean values for the 4 cm^2 cells

	$\bar{m}_{4\text{ cm}^2} (\%/\Omega\text{ cm}^2)$	$\overline{\text{PFF}}_{4\text{ cm}^2} (\%)$
Mean values	-4.9 ± 0.6	83.4 ± 0.6
R_{S} -method	$m_{\text{fit}} (\%/\Omega\text{ cm}^2)$	$\text{FF}_{0,\text{fit}} (\%)$
$R_{\text{S,int. var.}}$	-5.0 ± 0.3	82.9 ± 0.4
$R_{\text{S,Suns}}$	-4.9 ± 0.3	83.6 ± 0.4
$R_{\text{S,light,dark,corr}}$	-5.2 ± 0.3	83.6 ± 0.4
$R_{\text{S,integral}}$	-5.5 ± 0.1	83.7 ± 0.2
$R_{\text{S,dark}}$	-6.2 ± 0.7	81.9 ± 0.5

Table 2

Slopes and FF-axis intersection points determined by a linear fit to the FF vs. R_S plot, in comparison with calculated mean values for the 150 cm^2 cells

	$\bar{m}_{150\text{ cm}^2} (\%/\Omega\text{ cm}^2)$	$\overline{\text{PFF}}_{150\text{ cm}^2} (\%)$
Mean values	-4.9 ± 0.1	82.8 ± 0.2
$R_{S,\text{method}}$	$m_{\text{fit}} (\%/\Omega\text{ cm}^2)$	$\text{FF}_{0,\text{fit}} (\%)$
$R_{S,\text{int. var.}}$	-5.2 ± 0.1	82.5 ± 0.2
$R_{S,\text{Suns}}$	-5.3 ± 0.1	83.5 ± 0.2
$R_{S,\text{light_dark,corr}}$	-5.1 ± 0.1	82.6 ± 0.1
$R_{S,\text{integral}}$	-7.3 ± 0.2	84.1 ± 0.3
$R_{S,\text{dark}}$	-10.4 ± 3.9	81.9 ± 2.3
$R_{S,\text{integral_modif.}}$	-5.5 ± 0.7	82.9 ± 0.9

expected and the fitted values, and hence, the lowest accuracy.

- (iii) Based on this first evaluation, we would suggest choosing the Suns- V_{OC} method for the determination of $R_{S,\text{light}}$ of small size solar cells, because the differences between the mean values for $\bar{m}_{4\text{ cm}^2}$ and $\overline{\text{PFF}}_{4\text{ cm}^2}$ to the fit parameter m_{fit} and $\text{FF}_{0,\text{fit}}$ are the smallest. Additionally, the Suns- V_{OC} measurement offers not only a method for the $R_{S,\text{light}}$ determination, but also very useful information e.g. the pseudo-fill factor and efficiency.

For the $12.5 \times 12.5\text{ cm}^2$ batch the same comparison of the parameters of the linear FF vs. R_S fit between the calculated and the experimentally determined values for each method has been performed, as for the 4.0 cm^2 cells above. The resulting values are displayed in Table 2. For this analysis the best correspondence is achieved by the corrected comparison of the dark and illuminated IV-curve, followed by the illumination intensity variation and the Suns- V_{OC} vs. one-sun IV-curve comparison method. The series resistance determined by the comparison of the Suns- V_{OC} with the one-sun IV-curve results in slightly higher values. The integration method shows a relatively large deviation from the calculated values. Again the $R_{S,\text{dark,fit}}$ method delivers unsatisfactory results.

4.3. Influence of an intended increase in recombination currents on the $R_{S,\text{light}}$ determination and improvement in the integration method

To check the robustness of the methods we added scratches on the front surface into the emitter layer, parallel to the fingers of the same solar cells that had been investigated before. This causes an increase in the loss currents, i.e. an increased space-charge region recombination current density J_{02} . Since no parameter that influences $R_{S,\text{light}}$ had been directly changed, we expect the changes in this value to be negligible for this investigation. After the $R_{S,\text{light}}$ values were measured with each method, the

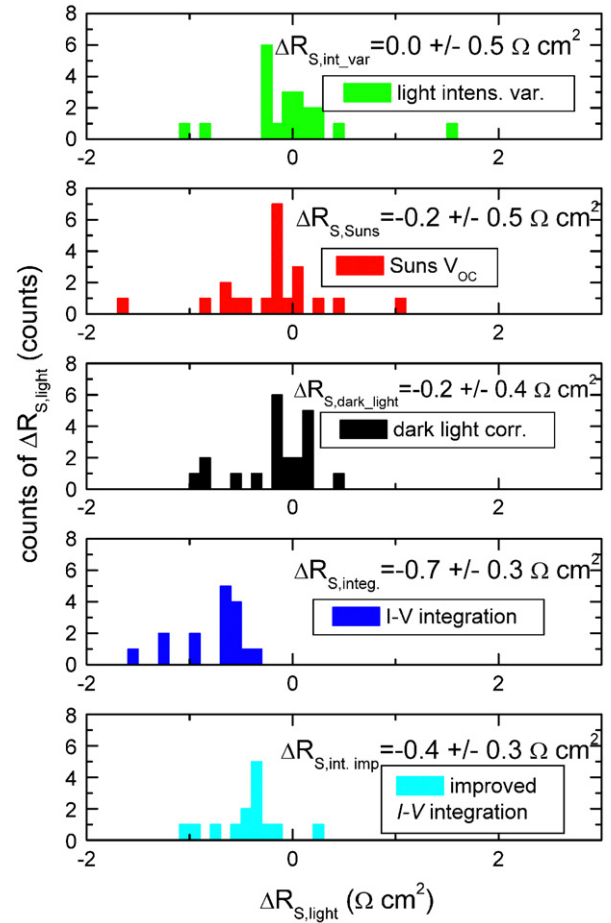


Fig. 8. The five histograms present the distribution of the $\Delta R_{S,\text{light}} = R_{S,\text{light,before}} - R_{S,\text{light,after}}$ values in 0.1 cm^2 intervals for each $R_{S,\text{light}}$ determination method for the 4 cm^2 cells.

deviation $\Delta R_{S,\text{light}} = R_{S,\text{light,before}} - R_{S,\text{light,after}}$ between these two states was determined and their mean value and standard deviation were calculated for both batches (see Fig. 8 (4.0 cm^2 cells) and Fig. 9 (150 cm^2 cells)).

From the data shown in Fig. 8 (4.0 cm^2) it is possible to conclude that the integration method is strongly influenced by shunt currents. The apparent $R_{S,\text{light,after}}$ values are all higher than the $R_{S,\text{light,before}}$. This can be explained, since the scratches influence the IV-curve by reducing the area under it and due to Eq. (9) the $R_{S,\text{integral}}$ value increases. The integration method determines an effective series resistance over the whole IV-curve, and thus it only delivers reliable values if there are no other effects but R_S that influence the FF significantly. All the other three methods for $R_{S,\text{light}}$ determination do not show such an obvious trend.

Due to the just-mentioned results of the small size solar cells (see Fig. 8) for the integration method, we developed an improvement of this method and evaluated it on both batches. To reduce the sensitivity of this method on the non-series resistance reduction of the area A , we suggest considering only a part of this area \bar{A} , which is less influenced by other loss mechanisms except from

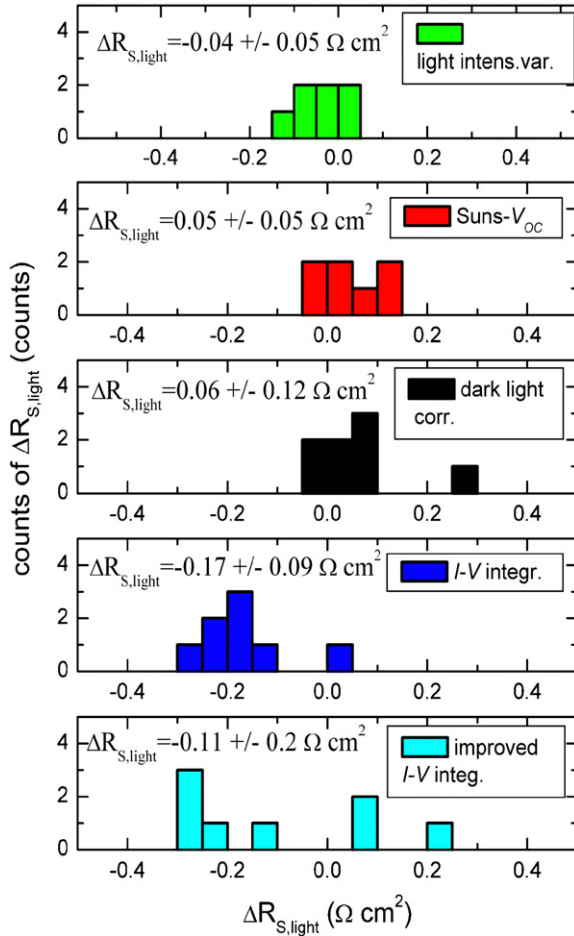


Fig. 9. The five histograms show the distribution of the $\Delta R_{S,\text{light}} = R_{S,\text{light,before}} - R_{S,\text{light,after}}$ values in $0.05 \Omega \text{ cm}^2$ intervals for each $R_{S,\text{light}}$ determination method for the 150 cm^2 cells.

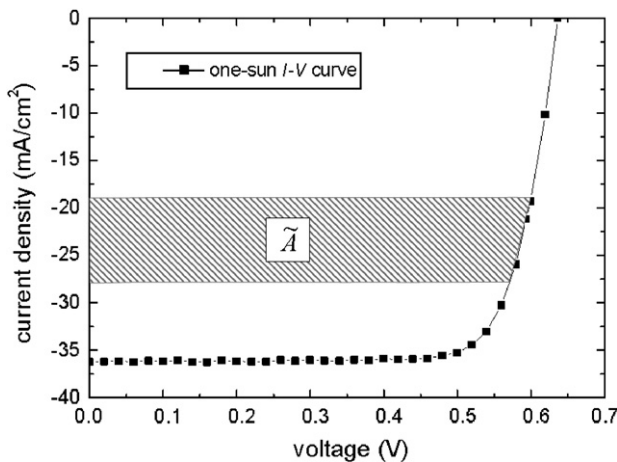


Fig. 10. This figure shows the partial area \tilde{A} of the modified integration method.

$R_{S,\text{light}}$ (see Fig. 10). By changing the integration borders in Eq. (8) to $J_1 = J_{\text{mpp}} + b_1$ and $J_2 = J_{\text{mpp}} + b_2$, calculating the integral and solving it for R_S we obtain the

following equation:

$$R_{S,\text{integ.imp.}} = \frac{2}{b_1^2 - b_2^2 + J_{\text{mpp}}(b_1 - b_2)} \times \left[\tilde{A} - \frac{nk_B T}{q} \left\{ \begin{aligned} &(b_1 - b_2) \\ &+ (J_{\text{SC}} + J_{\text{mpp}}) \ln \left(\frac{J_{\text{SC}} - b_1 - J_{\text{mpp}}}{J_{\text{SC}} - b_2 - J_{\text{mpp}}} \right) \\ &- b_1 \ln \left(\frac{J_{\text{SC}} - b_1 - J_{\text{mpp}}}{J_0} \right) \\ &+ b_2 \ln \left(\frac{J_{\text{SC}} - b_2 - J_{\text{mpp}}}{J_0} \right) \end{aligned} \right\} \right] \quad (15)$$

Variation of the parameters b_1 and b_2 have shown that the best results can be achieved with $b_1 = -10 \text{ mA/cm}^2$ and $b_2 = -15 \text{ mA/cm}^2$. Figs. 8 and 9 (bottom) show the $\Delta R_{S,\text{light}} = R_{S,\text{light,before}} - R_{S,\text{light,after}}$ distribution of the improved integration method $R_{S,\text{integ.imp.}}$, including mean values and standard deviation. For the 4 cm^2 cells the improvement is obvious. The modification of the integration method is also an improvement for the 150 cm^2 cells, as can be seen by the lower mean value of $\Delta R_{S,\text{integ.imp}}$ compared with $\Delta R_{S,\text{integ}}$ values before the modification (see Fig. 9). However, this improvement is accompanied by an increase in the standard deviation, which can be explained by lowering the smoothing characteristic of the integral due to the reduction in the area.

Coming back to the robustness check, both solar cell sizes show very similar behavior. The least affected method is the illumination intensity variation, closely followed by the comparison of the corrected dark-illuminated method and the Suns- V_{OC} vs. one-sun I - V -method (Figs. 8 and 9). Thus, all these three methods seem to be similarly robust. A higher statistical sample would be recommended to determine the best of these methods.

5. Discussion

As expected from the theory [2] the $R_{S,\text{dark}}$ method delivers wrong values for solar cell characterization under operating conditions, and is therefore not recommended.

In Fig. 7 the $R_{S,\text{integral}}$ values show very good agreement with the other $R_{S,\text{light}}$ determination methods for $R_S < 1.0 \Omega \text{ cm}^2$, but they tend to underestimate the series resistance with rising values. This trend might be explained by the following two aspects: (1) the integration method determines an effective series resistance value over the whole I - V -curve; and (2) the series resistance is approximately constant at different current densities/illuminations, as long as the sheet resistance of the base surpasses the emitter sheet resistance and/or $J R_S < nk_B T/q$, otherwise the series resistance declines from its maximum at the maximum power point to its lowest value at open-circuit voltage conditions. Thus, if one of the prerequisites mentioned under (2) is not fulfilled, an underestimated $R_{S,\text{light}}$ value is the consequence, due to the first aspect [9]. The second assumption is fulfilled for $J = 32 \text{ mA/cm}^2$ and

$R_S < 0.8 \Omega \text{ cm}^2$, which is in quite good agreement with the observations made (see Fig. 7). As this method is also very sensitive to an increase in recombination currents, and thus results in too low R_S values; we also do not recommend this method for solar cell characterization.

In spite of the very good results of the remaining $R_{S,\text{light}}$ determination methods there are some advantages and disadvantages of each method which will be discussed in the following.

For the Suns- V_{OC} method, problems may occur due to the different measuring setups, producing spectral mismatch between the spectral irradiance of the flash and the steady-state sun simulator, as both measurements are performed with different contacting features. On the one hand, this method has the advantage of delivering the very useful and interesting pseudo fill factor and pseudo-efficiency value. However, on the other hand, J_{SC} , base resistivity and solar cell thickness need to be known to obtain maximum accuracy using the generalized correction.

The main drawback of the intensity variation method is the subjective choice of the parameter ΔJ which results in slightly different $R_{S,\text{light}}$ values. These are also pretty sensitive to different measurement point densities of the IV -curve and the choice of their interpolation function type. By choosing the different illumination intensities very close to the one-sun intensity, the actual working conditions of the cell are best simulated, but the difference between the different V_i values declines, resulting in a higher uncertainty of the linear fit of the $[V_i, J_i]$ values. This can be compensated by a high repetition of measurements of each V_i and calculating its mean value, as proposed by Altermatt [14]. This procedure determines the series resistance very accurately, but is also very time consuming and hence only practicable for lab measurements. Subsequently based on the investigations carried out in this work it can be concluded that the intensity variation method performs very well.

The corrected light dark IV -curve comparison method showed also very good results for all measurements carried out in this work. It is a simple and quick procedure. However, it is important that the same measurement setup with the exact same contacting properties is used for all required IV -curves of each solar cell (as by the intensity variation method). A probably small but still critical point of this procedure to determine the $R_{S,\text{light_dark_corr}}$ value is that an error could occur due to the correction of Eq. (2) with $R_{S,\text{dark}}$ determined at the short circuit current density J_{SC} (see Eq. (4)), because $R_{S,\text{dark}}$ is dependent on the current density [9]. It would be more accurate to determine the $R_{S,\text{dark}}$ at a current density around $J = J_{SC} - J_{mpp}$, where the voltage difference between the light and the dark IV -curve is determined for $R_{S,\text{light_dark_corr}}$ calculation.

To conclude the discussion, we can divide the five methods under investigation into two groups:

1st group: The dark-fit (see Section 2.1) and the integral (see Section 2.5) method are based on the one and two diode models, respectively.

2nd group: The other three methods (see Sections 2.2–2.4) are based on a comparison of a one-sun IV -curve with another or more IV -curves under different illumination conditions.

The methods of the first group, rely on the model parameters in the equation describing the solar cell device physics and data. As such, these methods may not be general with respect to cells with three-dimensional effects, lumped series resistance, high-level injection in the substrate etc., where the solar cells do not behave as ideal diodes with the ideality factors $n_1 = 1$ and $n_2 = 2$ and the constant R_P and R_S as implemented in the fits.

The methods of the second group are all based on the same principle. The same net dark current is supplied (generated by a combination of photons and electrons) to the device at two different combinations of light and terminal current. These methods do not require detailed models or curve fits. So these three methods are somewhat similar and rather independent of the model assumptions such as ideality factor, lumped series resistance, etc. In rating these three methods by theoretical considerations, the intensity-variation method evaluates R_S under operating condition very close to the device's operating point (uniform illumination and J_{mpp}). Suns- V_{OC} is next closest (uniform illumination but no terminal current and low intensity for the reference case). The light–dark IV -curve comparison method is, from these three methods, the farthest from the operating point, with the sign of the current (and voltage drops) slightly reversed from J_{mpp} , and there is no light at all for the reference case.

6. Conclusion

Five different series resistance methods have been reviewed in detail. The goal of this work was to determine the most reliable and robust method for $R_{S,\text{light}}$ measurement by two different investigations. Firstly, by comparing the linear fit parameters of a FF vs. R_S plot with the corresponding calculated values for the slope m and FF-axis intersection point (accuracy check), and secondly, by comparing $\Delta R_{S,\text{light}} = R_{S,\text{light,before}} - R_{S,\text{light,after}}$ values after putting scratches into the surface of the solar cell and increasing the shunt and space-charge region recombination current densities (robustness check). For small size solar cells all $R_{S,\text{light}}$ determination methods perform similarly well. However, it has been shown that the integral method can be strongly influenced by the increased recombination currents. We improved this method in order to make it less sensitive to non-series-resistance effects. Subsequently, it is possible to conclude that for both, small and big solar cells the illumination intensity variation, the comparison of a Suns- V_{OC} with a one-sun IV -curve and the corrected dark-illuminated comparison methods appear to be least affected by an increase in recombination current densities, and deliver also the most reliable values compared with the expected average values for the slope of the FF vs. R_S plot. Thus, these three methods seem to be the most reliable and robust methods to determine the series resistance out of the methods under

investigation. The fit of the dark IV -curve results in far too low series resistance values, whereas the integration method is strongly affected by increased recombination currents, and are therefore not recommended for solar cell characterization.

Acknowledgment

The authors thank E. Schäffer, T. Roth, S. Rein, E. Barrigón, A. Leimenstoll and M. Hermle for measurement instructions, solar cell processing and characterization, and A. Cuevas for fruitful discussion.

This work has been supported by the German Federal Ministry for the Environment, Nature Conservation and Nuclear Safety (BMU) under Contract no. 0329960.

References

- [1] L.D. Nielsen, IEEE Trans. Electron Devices ED- 29 (1982) 821.
- [2] A.G. Aberle, S.R. Wenham, M.A. Green, Proceedings of the 23rd IEEE Photovoltaic Specialists Conference, Louisville, Kentucky, USA, IEEE, New York, 1993, p. 133.
- [3] A. Rohatgi, J.R. Davis, R.H. Hopkins, et al., Solid-State Electron. 23 (1980) 415.
- [4] J. Dicker, Dissertation Thesis, University of Konstanz, Germany, 2003, p. 129.
- [5] M. Wolf, H. Rauschenbach, Adv. Energy Convers. 3 (1963) 455.
- [6] R.A. Sinton, A. Cuevas, Proceedings of the 16th European Photovoltaic Solar Energy Conference, Glasgow, UK, James & James, London, 2000, p. 1152.
- [7] R.J. Handy, Solid-State Electron. 10 (1967) 765.
- [8] European Standard, ES 60891, 1994, IEC 891:1987+A1:1992.
- [9] A. Cuevas, G.L. Araújo, J.M. Ruiz, Proceedings of the Fifth European Photovoltaic Solar Energy Conference, Athens, Greece, Reidel, Dordrecht, 1983, p. 114.
- [10] L.D. Swanson, private communication with M. Wolf and H. Rauschenbach (see [5]).
- [11] G.L. Araújo, E. Sánchez, IEEE Trans. Electron Devices ED-29 (1982) 1511.
- [12] A. Mette, C. Schetter, D. Wissen, S. Lust, S.W. Glunz, G. Willeke, Proceedings of the Fourth World Conference on Photovoltaic Energy Conversion, Hawaii, USA, IEEE, Hawaii, 2006.
- [13] K.B. Böer, R.M. Swanson, R.A. Sinton, Advances in Solar Energy, vol. 6, Plenum Press, New York, 1990, p. 438.
- [14] P.P. Altermatt, G. Heiser, A. Aberle, A. Wang, J. Zheo, S.J. Robinson, S. Bowden, M. Green, Prog. Photovolt. 4 (1996) 399.